Supplementary Information

for

Developing Tough, Fatigue-Resistant and Conductive Hydrogels by In-Situ Growing Metal Dendrites

Mengjie Si [a, +], Yueman Tang [a, +], Chen Xu [a], Chen Yu Li [b, *], Kaishun Xia [c], Wei Xu [d], Ji Lin [e], Zhen Jiang [f], Jintao Yang [a], and Si Yu Zheng [a, *]

[a] College of Materials Science & Engineering, Zhejiang University of Technology, Hangzhou 310014, P. R. China

[b] Research Center for Humanoid Sensing, Zhejiang Lab, Hangzhou 311100, P. R. China

[c] Department of Orthopedics, The Second Affiliated Hospital, Zhejiang University, Hangzhou, 310009, P. R. China

[d] ZJU-Hangzhou Global Scientific Center, Zhejiang University, Hangzhou 311200, P. R. China

[e] School of Mechanical Engineering & Mechanics, Ningbo University, Ningbo 315211, P. R. China

[f] School of Mechanical Materials, Mechatronic and Biomedical Engineering, University of Wollongong, Wollongong, NSW 2522, Australia

[+] These authors contributed equally to this work.

* E-mail of corresponding author: Chen Yu Li (lcyzju@163.com) and Si Yu Zheng (zhengsiyu@zjut.edu.cn)

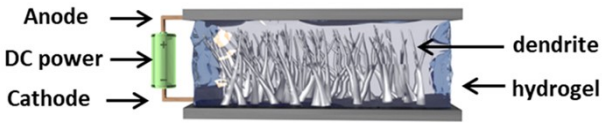

Fig. S1. Schematic diagram to present the method to grow Sn dendrites in gel.

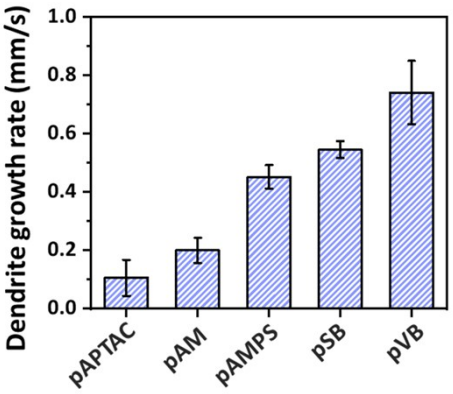

Fig. S2. Dendrite growth rates in hydrogels with different polymer structures at 10 V (Concentration of $SnCl_2$ solution: 2 M).

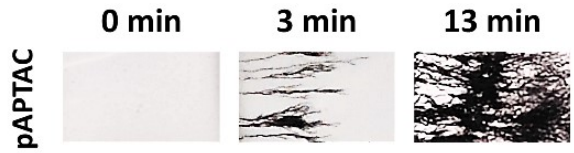

Fig. S3. Image of pAPTAC gel after growing Sn dendrite for different time at 10 V.

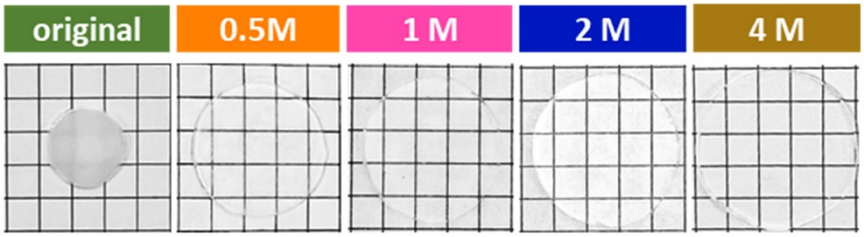

Fig. S4. Digital images of pVB gel after swelling in $SnCl_2$ solution with different concentrations.

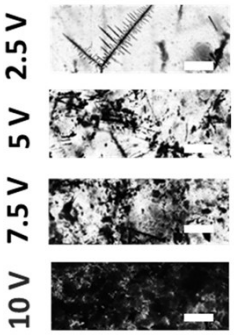

Fig. S5. Polarizing microscopic images to show the dendrites grown density in gel at different voltages after growing for 80 s.

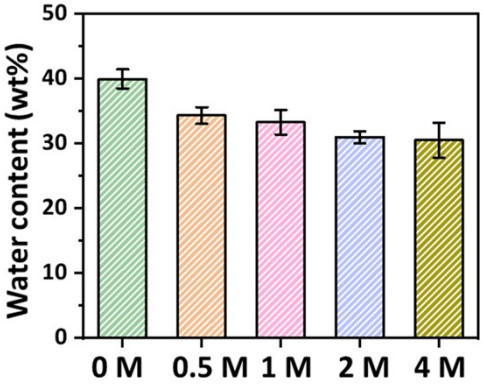

Fig. S6. The water content of pVB@xSn gels, prepared by swelling in $SnCl_2$ solution with different concentrations and then balanced in water.

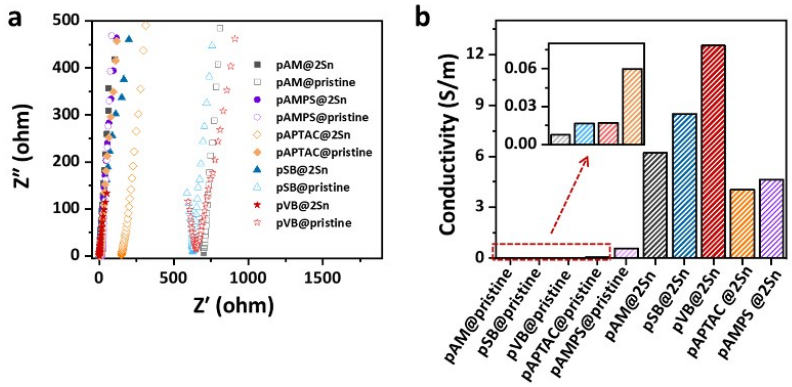

Fig. S7. The (a) EIS spectroscopy and (b) conductivity of pristine/dendrite composite gels with different molecular structures.

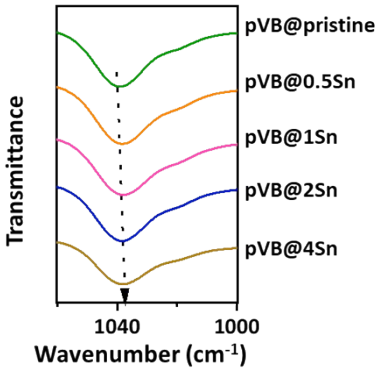

Fig. S8. FTIR spectra of pVB@pristine and pVB@xSn gels (x=0.5, 1, 2 and 4).

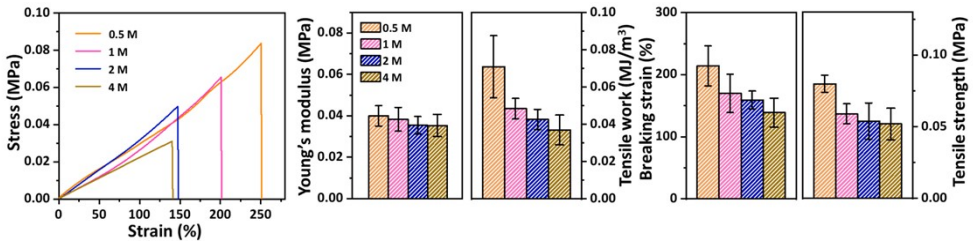

Fig. S9. The tensile stress-strain curves of pVB gels after swelling in $SnCl_2$ solutions with different concentrations; corresponding Young's modulus, tensile work, breaking strain and tensile strength.

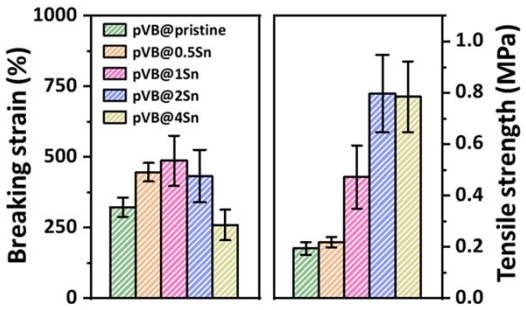

Fig. S10. Calculated tensile strength and breaking strain of pVB@xSn gels after equilibrium in water.

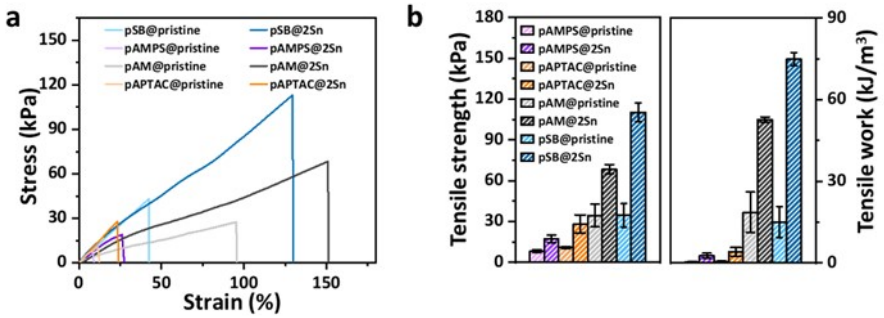

Fig. S11. (a) Tensile curves of dendrite composite gels with different molecular structures, and (b) the corresponding tensile strength and tensile work.

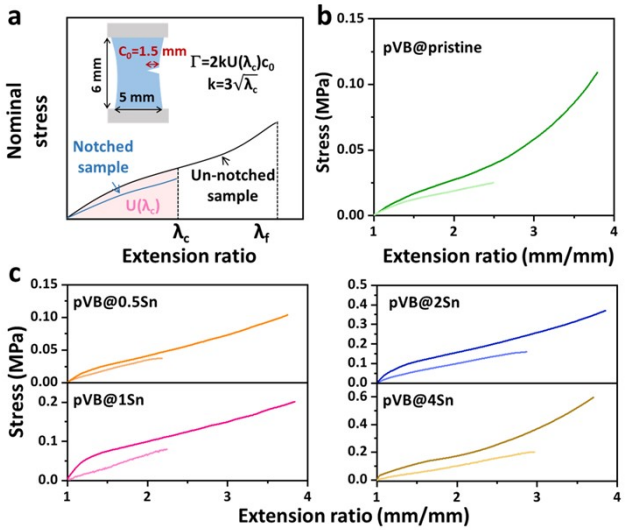

Fig. S12. (a) Method for evaluating fracture toughness using a single notch test. (b, c) Stress-extension ratio curves of (b) pVB@pristine and (c) pVB@xSn gels with/without notch in single notched sample tests.

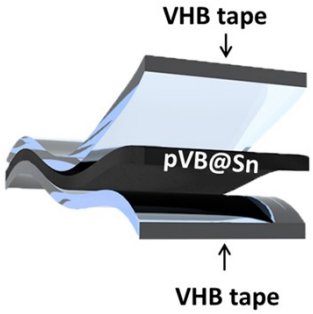

Fig. S13. Schematic to illustrate the structure of pVB@2Sn gel based sensor.

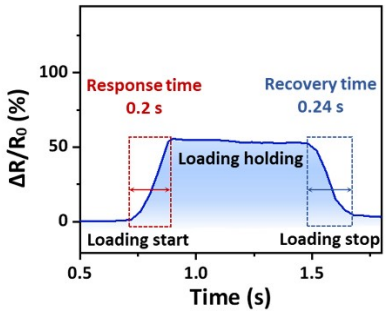

Fig. S14. Response and recovery time of the pVB@2Sn gel sensor under 20% strain.

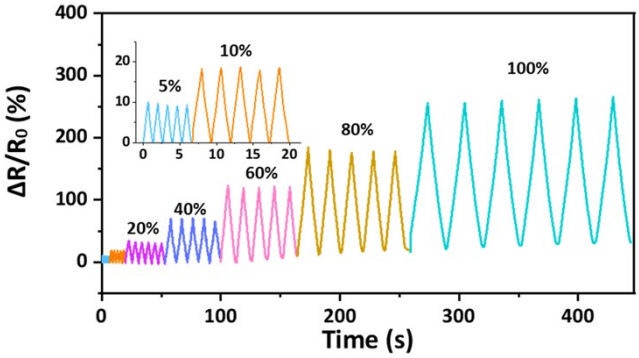

Fig. S15. The resistive signal of a notched pVB@2Sn gel sensor under different applied strains ranging from 5% to 100%.

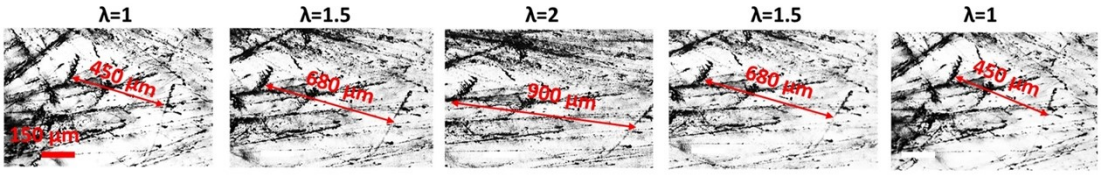

Fig. S16. Polarizing microscopic images to show the morphology change of dendrite network under loading and unloading states.

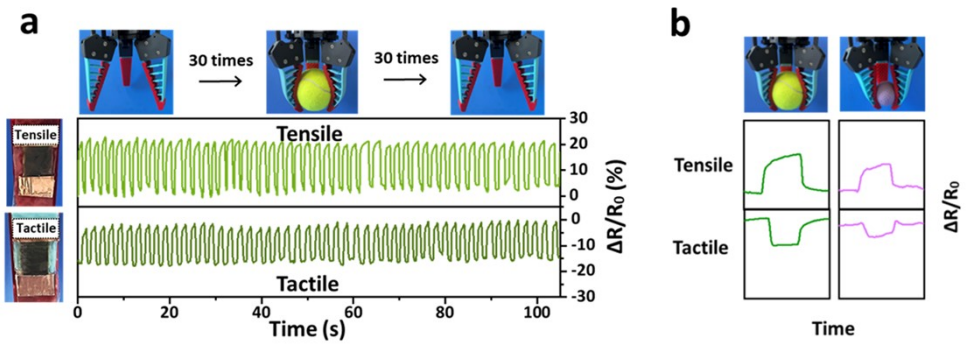

Fig. S17. (a) Two channel mode sensing the grasping and releasing action of mechanical claw by using pVB@2Sn sensor. (b) The two-channel signals of the sensor during grasping items with different sizes.

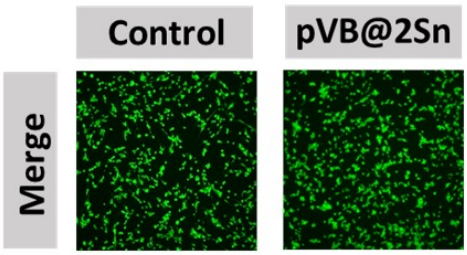

Fig. S18. The biocompatibility of pVB@2Sn gel.

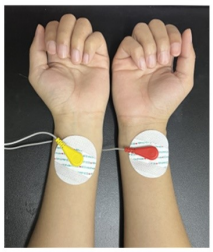

Fig. S19. Image of the experimental setup for ECG monitoring.

Table S1. Recipe for preparing different hydrogels.

	Monomer	Initiator	Crosslinker	Water
pVB	1.22 g	0.01 g	0.003 g	0.97 g
pSB	1.11 g			1.08 g
pAM	0.28 g			1.91 g
pAPTAC	1.10 g			1.09 g
pAMPS	0.83 g			1.23 g